npg

Apoptotic microtubules delimit an active caspase free area in the cellular cortex during the execution phase of apoptosis

M Oropesa-Ávila[1], A Fernández-Vega[1], M de la Mata[1], JG Maraver[1], MD Cordero[2], D Cotán[1], M de Miguel[2], CP Calero[1], MV Paz[1], AD Pavón[1], MA Sánchez[1], AP Zaderenko[3], P Ybot-González[4] and JA Sánchez-Alcázar*[1]

Apoptotic microtubule network (AMN) is organized during apoptosis, forming a cortical structure beneath plasma membrane, which has an important role in preserving cell morphology and plasma membrane permeability. The aim of this study was to examine the role of AMN in maintaining plasma membrane integrity during the execution phase of apoptosis. We demonstrated in camptothecin-induced apoptosis in H460 cells that AMN delimits an active caspase free area beneath plasma membrane that permits the preservation of cellular cortex and transmembrane proteins. AMN depolymerization in apoptotic cells by a short exposure to colchicine allowed active caspases to reach the cellular cortex and cleave many key proteins involved in plasma membrane structural support, cell adhesion and ionic homeostasis. Cleavage of cellular cortex and plasma membrane proteins, such as α-spectrin, paxilin, focal adhesion kinase (FAK), E-cadherin and integrin subunit $\beta4$ was associated with cell collapse and cell detachment. Otherwise, cleavage-mediated inactivation of calcium ATPase pump (PMCA-4) and Na^+/Ca^{2+} exchanger (NCX) involved in cell calcium extrusion resulted in calcium overload. Furthermore, cleavage of Na^+/K^+ pump subunit β was associated with altered sodium homeostasis. Cleavage of cell cortex and plasma membrane proteins in apoptotic cells after AMN depolymerization increased plasma permeability, ionic imbalance and bioenergetic collapse, leading apoptotic cells to secondary necrosis. The essential role of caspase-mediated cleavage in this process was demonstrated because the concomitant addition of colchicine that induces AMN depolymerization and the pan-caspase inhibitor z-VAD avoided the cleavage of cortical and plasma membrane proteins and prevented apoptotic cells to undergo secondary necrosis. Furthermore, the presence of AMN was also critical for proper phosphatidylserine externalization and apoptotic cell clearance by macrophages. These results indicate that AMN is essential to preserve an active caspase free area in the cellular cortex of apoptotic cells that allows plasma membrane integrity during the execution phase of apoptosis.

Apoptosis is a physiologic mechanism employed by most multicellular organisms to maintain tissue remodeling during development, tissue homeostasis, removal of senescent cells and the elimination of cells with severe genetic damage.[1] Moreover, many antineoplasic drugs such as campothecin, a topoisomerase I inhibitor, kill tumor cells by inducing apoptosis. This mechanism of cell death is thought to be physiologically advantageous because apoptotic cells are removed by phagocytosis before they lose their permeability barrier, thus preventing induction of an inflammatory response to the dying cells. In apoptosis, all the degradative processes are isolated from the extracellular space by the plasma membrane, which remains impermeable. However, the mechanisms of how plasma membrane and associated proteins are protected from the action of caspases are not known. In contrast, necrosis is accompanied by disruption of plasma membrane integrity so all intracellular compounds are released to the intercellular space, thus inducing inflammation and more toxic effects to adjacent cells.[2,3] In contrast to apoptotic cells *in vivo*, cells which undergo apoptosis *in vitro* cannot usually be cleared by phagocytes and undergo a late process of secondary necrosis defined as a loss of cell membrane integrity, calcium influx from the medium and release of cell content into the extracellular space.[4] Previous evidence suggests that the actomyosin cytoskeleton has an essential role in apoptotic cell remodeling during the early

[1]Centro Andaluz de Biología del Desarrollo (CABD-CSIC-Universidad Pablo de Olavide), and Centro de Investigación Biomédica en Red: Enfermedades Raras, Instituto de Salud Carlos III, Sevilla, Spain; [2]Departamento de Citología e Histología Normal y Patológica, Facultad de Medicina. Universidad de Sevilla, Sevilla, Spain; [3]Sistemas Físicos, Químicos y Naturales-Universidad Pablo de Olavide, Sevilla, Spain and [4]Instituto de Biomedicina de Sevilla (IBIS)-CSIC, Hospital Virgen del Rocío, Sevilla, Spain
*Corresponding author: JA Sánchez Alcázar, Centro Andaluz de Biología del Desarrollo (CABD). Consejo Superior de Investigaciones Científicas. Universidad Pablo de Olavide, Carretera de Utrera Km 1, Sevilla 41013, Spain. Tel: 349 5497 8071; Fax: 349 5434 9376; E-mail: jasanalc@upo.es

events of the execution phase, whereas all other cytoskeleton elements (microtubules and intermediate filaments) are dismantled.[5] However, during the course of the execution phase, the actomyosin filaments are also depolymerized by a caspase-dependent mechanism. In this situation apoptotic cell formed a network of apoptotic microtubules as the main cytoskeleton element of the apoptotic cell. The presence of microtubules in apoptotic cells has previously been reported.[6,7] Moreover, more recent results indicate that microtubules during apoptosis assist in the dispersal of nuclear and cellular fragments,[8,9] and may help to preserve the integrity of plasma membrane of the dying cell.[10]

The aim of this study was to examine the role of AMN in preserving plasma membrane integrity during the execution phase of apoptosis. Our results suggest that AMN works as a physical barrier keeping an active caspase free area in the cellular cortex of apoptotic cells, and thus avoiding the cleavage of essential proteins in maintaining plasma membrane integrity.

Results

AMN works as a physical barrier against active caspases. To examine the disposition of microtubules during apoptosis and its relationship with plasma membrane, cells were fixed and stained for β-tubulin, plasma membrane and active caspase-3 (Figures 1a and b). Both attached apoptotic cells and floating cells, which represent apoptotic cells in secondary necrosis were analyzed. We also examined apoptotic cells treated with colchicine for 1 h or colchicine plus the pan-caspase inhibitor z-VAD to examine the effect of AMN depolymerization when caspases were active or inhibited (Figures 1a and b). In apoptotic cells, AMN seemed to work as a physical barrier impeding active caspases to reach the cellular cortex and plasma membrane. The cellular cortex, which appears as a narrow area between the plasma membrane and the apoptotic microtubules was free of active caspase-3. On the contrary when AMN was depolymerized by colchicine, active caspase-3 reached freely the cellular cortex and plasma membrane. Likewise, the active caspase-3 free area in the cellular cortex disappeared in apoptotic cells treated with colchicine and the pan-caspase inhibitor z-VAD and in floating death cells without AMN that represent cells in secondary necrosis. As expected, control cells without treatment and control cells treated with colchicine for 1 h were not apoptotic and did not show activation of caspase-3.

For a better visualization of AMN structure in genuine apoptotic cells we performed a 3D reconstruction with the Delta Visión software of cells stained for microtubules, actin and nuclei. We found that apoptotic cells with fragmented nuclei lacked actin microfilaments and AMN presented the typical 'cocoon' like structure that may function as a protective barrier surrounding the whole-cell (Supplementary Figure S1).

AMN prevents plasma membrane permeability. To assess the significance of the AMN in genuine apoptotic cells *versus* apoptotic cells without AMN, we examined plasma membrane permeability in both apoptotic cells and cells in secondary necrosis. We also analyzed apoptotic cells treated with colchicine for 1 h or colchicine plus the pan-caspase inhibitor z-VAD to examine the effect of AMN depolymerization when caspases were active or inhibited. Cells were examined using the Dead Red reagent, a red fluorescent nucleic acid stain that only labels permeable cells, thus testing plasma membrane integrity.[11] We found that AMN was present in almost 100% of adherent apoptotic cells that were impermeable to the supravital dye (Figures 2a and b). However, we observed that membrane integrity was impaired in secondary necrotic cells, in which AMN was disorganized (Figures 2a and b). Interestingly, membrane permeability was also impaired in apoptotic cells, in which AMN was disorganized after colchicine treatment. However, plasma membrane remained impermeable in apoptotic cells treated simultaneously with colchicine and z-VAD, suggesting that although active caspases were able to reach the cellular cortex after AMN disorganization by colchicine, functional active caspases and consequently cleavage of cellular cortex and plasma membrane proteins are necessary to impair plasma membrane permeability. As expected, control cells without treatment and control cells treated with colchicine for 1 h remained impermeable. These observations were quantified scoring the proportion of living (impermeable and non-apoptotic nuclei), apoptotic (impermeable and fragmented nuclei) and secondary necrotic cells (permeable and fragmented nuclei) under the different experimental conditions (Figure 2b).

Plasma membrane and cell cortex proteins are protected from caspase-mediated cleavage by AMN. To verify the functional relevance of AMN as a physical barrier during the execution phase of apoptosis, we examined the integrity of well-known cytosolic, nuclear, cellular cortex and plasma membrane proteins which are common substrates of effector caspases, in control, apoptotic and secondary necrotic cells. Apoptotic cells were also treated with colchicine or colchicine plus the pan-caspase inhibitor z-VAD for 1 h to examine the effect of AMN depolymerization when caspases were active or inhibited (Figure 3). Western blot analysis revealed that initiator caspase-9 and efector caspases-3 and -7 were activated and nuclear (PARP and lamin B) and cytosolic proteins (cytokeratins 5/8, cytokeratin 18 and ROCK-1) were cleaved in genuine apoptotic cells with AMN indicating that caspases were degrading nuclear and cytosolic components during the execution phase of apoptosis. On the contrary, cellular cortex and plasma membrane proteins such as α-spectrin, paxilin, focal adhesion kinase (FAK), E-cadherin, integrin β4, plasma membrane Ca^{2+} ATPase (PMCA-4), Na^+-Ca^+ exchanger (NCX) and Na^+/K^+ pump subunit β, were intact in apoptotic cells with AMN. However, cellular cortex and transmembrane proteins were cleaved when AMN was disorganized in apoptotic cells by colchicine treatment or in secondary necrotic cells. As an exception, the plasma membrane protein Na^+/K^+ pump subunit α, was not cleaved after AMN disorganization, suggesting that this particular subunit has no cleavage sequence for caspases. The critical role of caspase-mediated cleavage of cellular cortex and transmembrane proteins after AMN depolymerization was demonstrated because their degradation was
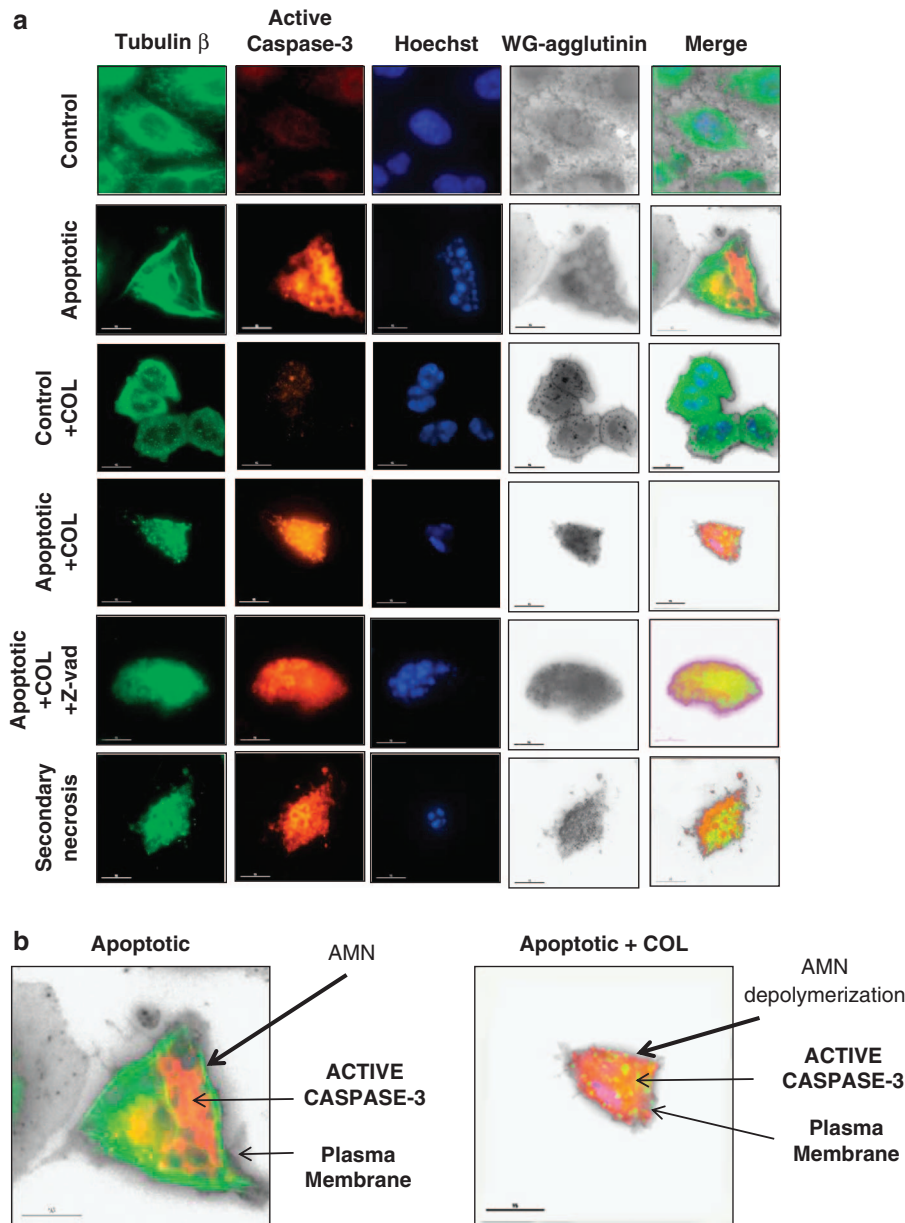
Figure 1 AMN during the execution phase of apoptosis. (**a**) Fluorescence microscopy of microtubules, plasma membrane and active caspase-3 in control cells, control cells treated with 2 μM colchicine (Control + COL), apoptotic cells, apoptotic cells treated with 2 μM colchicine (Apoptotic + COL) for 1 h or colchicine plus 50 μM z-VAD (Apoptotic + COL + z-VAD) for 1 h and cells in secondary necrosis. H460 cells were grown on glass coverslips and apoptosis was induced as is described in the enriched apoptotic assay in Materials and Methods. Secondary necrotic cells were collected from the floating cells in de medium after the treatment and cytospined on a slide. Apoptotic cells were treated with colchicine or colchicine plus the pan-caspase inhibitor z-VAD to examine the effect of AMN depolymerization when caspases were active or inhibited. Then, cells were fixed and immunostained with anti-β-tubulin (green), anti-active caspase-3. Plasma membrane was revealed by staining with WG-agglutinin. Nuclear morphology was revealed by staining with Hoechst 33342 (1 μg/ml). Bar = 15 μm. (**b**) Magnification of apoptotic cells and apoptotic cells after 1 h of treatment with colchicine

prevented when z-VAD was added simultaneously with colchicine.

All together these data indicate that AMN in apoptotic cells encloses most of the cellular volume where active caspases are degrading cytosolic and nuclear proteins, keeping the cellular cortex and plasma membrane free of active caspases.

To confirm these data, we performed immunofluorescence analysis of cellular cortex and plasma membrane proteins to visualize its integrity in the presence or absence of AMN. As is

shown in Figure 4, PMCA-4 is a plasma membrane protein involved in calcium extrusion preserved in apoptotic cells with AMM but it was degraded when AMN was depolymerized by 1 h incubation with colchicine or in cells in secondary necrosis without AMN. PMCA-4 cleavage after AMN depolymerization was mediated by caspases because its degradation was prevented when z-VAD was added simultaneously with colchicine (Figure 4).

Likewise, FAK, another cellular cortex protein involved in cell adhesion complexes, was preserved in apoptotic cells
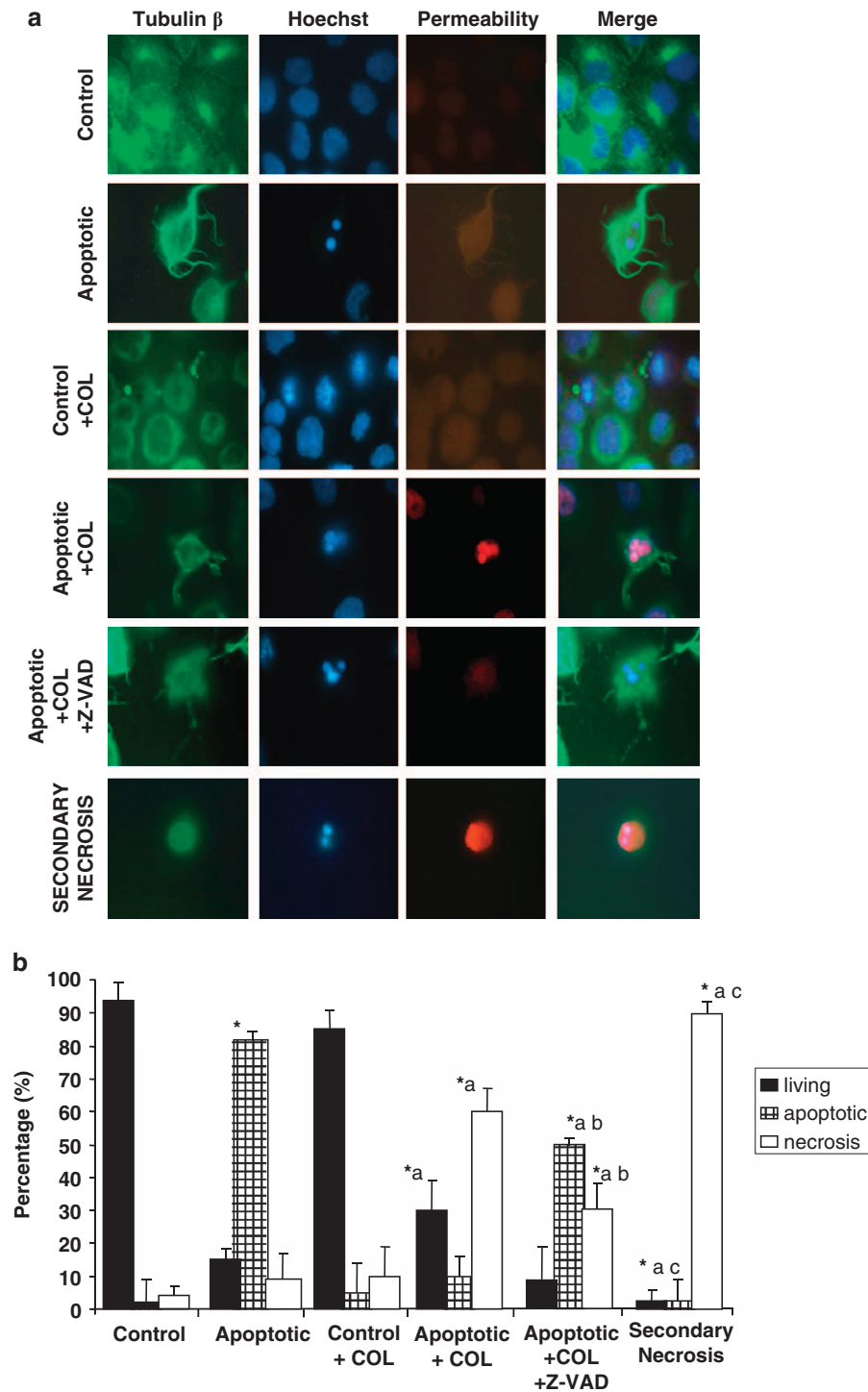
Figure 2 AMN and plasma membrane permeability. (**a**) Fluorescence microscopy of microtubules and plasma membrane permeability in control cells, control cells treated with 2 μM colchicine (Control + COL), apoptotic cells, apoptotic cells treated with 2 μM colchicine (Apoptotic + COL) for 1 h or colchicine plus 50 μM z-VAD (Apoptotic + COL + z-VAD) for 1 h and cells in secondary necrosis. H460 cells were grown on glass coverslips and apoptosis was induced as is described in the enriched apoptotic assay in Materials and Methods. Secondary necrotic cells were collected from the floating cells in de medium after the treatment and cytospined on a slide. Apoptotic cells were treated with colchicine or colchicine plus the pan-caspase inhibitor z-VAD to examine the effect of AMN depolymerization when caspases were active or inhibited. Before fixation cells were treated with the Dead Red dye, then fixed and immunostained with mouse anti-β-tubulin (green). Nuclear morphology was revealed by staining with Hoechst 33342 (1 μg/ml). Bar = 15 μm. (**b**) Proportion of living (black), apoptotic (hatched) and secondary necrosis (white) H460 cells, based on the cell and nuclear morphological characteristics and plasma membrane permeability. More than 100 cells were examined for each experimental condition. *$P < 0.01$ significant differences with respect to Control cells. [a]$P < 0.01$, significant differences with respect to Apoptotic cells. [b]$P < 0.01$, significant differences with respect to Apoptotic + COL. [c]$P < 0.01$, significant differences with respect to Apoptotic + COL + z-VAD treated cells
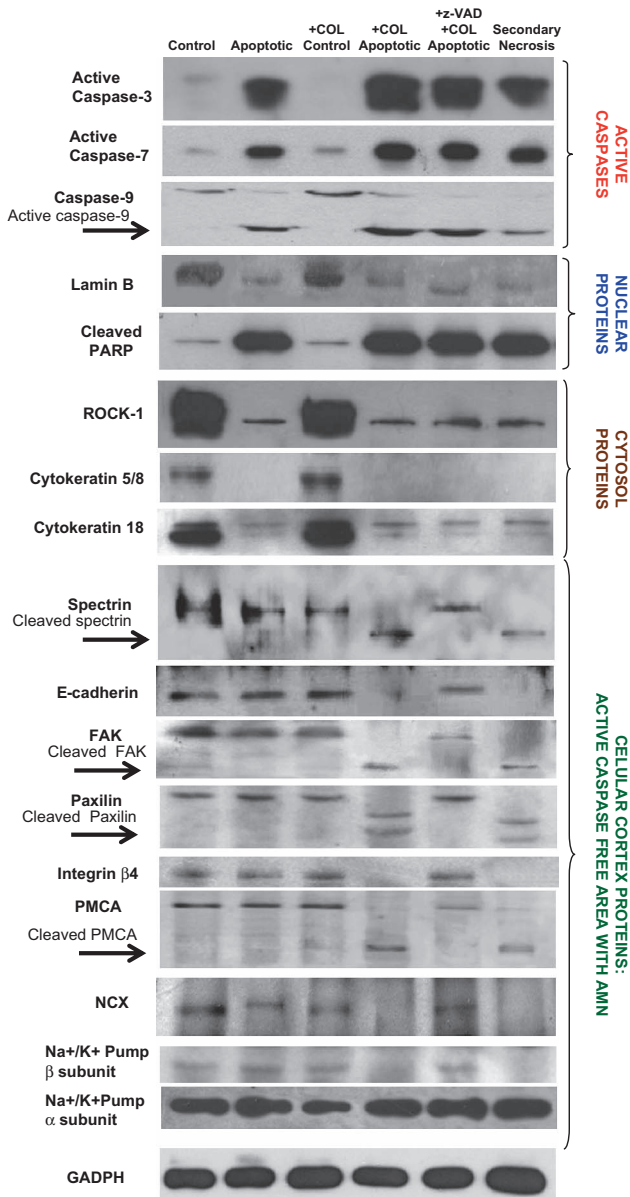
Figure 3 Western blotting analysis of nuclear, cytosolic and cellular cortex proteins in the execution phase of apoptosis. Western blotting of nuclear (PARP, lamin C), cytosolic (cytokeratin 5/8, cytokeratin 18 and ROCK-1) and cellular cortex proteins (spectrin, FAK, paxilin, integrin β4, E-cadherin, PMCA-4, NCX, anti-Na$^+$/K$^+$ pump subunit α and β, in control cells, control cells treated with 2 μM colchicine (Control + COL), apoptotic cells, apoptotic cells treated with 2 μM colchicine (Apoptotic + COL) for 1 h or colchicine plus 50 μM z-VAD (Apoptotic + COL + z-VAD) for 1 h and secondary necrotic cells. Apoptosis in H460 cells was induced as is described in the enriched apoptotic assay in Materials and Methods. Secondary necrotic cells were collected from the floating cells in de medium after the treatment. Apoptotic cells were treated with colchicine or colchicine plus the pan-caspase inhibitor z-VAD to examine the effect of AMN depolymerization when caspases were active or inhibited. Cell lysates from H460 cells were resolved by SDS-PAGE and protein levels and cleavage fragments were determined by western blotting. Equal loading and transfer were shown by repeat probing with anti-GADPH

with AMM but it was degraded when AMN was depolymerized by colchicine or in cells in secondary necrosis without AMN (Supplementary Figure S2).

Functional relevance of AMN in cell area and cell attachment. To examine whether AMN disorganization by colchicine, which allows the caspase-dependent cleavage of plasma membrane-cytoskeleton proteins such as spectrin and cell adhesion proteins such as paxilin, integrin β4, FAK and E-cadherin, was associated with cell collapse and substrate detachment, we measured cell area at the cell maximum perimeter and scored attached and floating cells in the medium in apoptotic cells with and without AMN. We found that AMN disorganization by 1 h of colchicine treatment induced a dramatic decreased in cell area and a significant increase in the number of floating cells (Figures 5a and b). Substrate detachment was prevented significantly in apoptotic cells after AMN disorganization by colchicine when caspases were inhibited by z-VAD suggesting the essential role of caspase-mediated cleavage of plasma membrane and cellular cortex proteins in this process. However, z-VAD was not able to prevent cell collapse after AMN depolymerization indicating that apoptotic microtubules *per se* are essential to maintain cell shape and morphology in apoptotic cells (Figure 5b). Likewise, colchicine treatment in control cells had not effect on cell attachment but it induced a significant reduction of cell area indicating that microtubules have an essential role in normal cell shape and morphology.

Cell content leakage, calcium and sodium overload, and bioenergetics collapse are prevented by AMN. To confirm whether AMN was responsible for maintaining cellular integrity in apoptotic cells, we measured LDH release (a cytosolic enzyme used as intracellular marker), intracellular calcium and sodium levels, mitochondrial membrane potential ($\Delta\psi$m) and ATP levels in control, apoptotic and secondary necrotic cells. Apoptotic cells were also treated with colchicine or colchicine plus the pan-caspase inhibitor z-VAD for 1 h to examine the effect of AMN depolymerization when caspases were active or inhibited. Figure 6a shows that LDH release was significantly increased in the culture medium of apoptotic cells after AMN disorganization by colchicine treatment and in secondary necrotic cells, indicating that the absence of AMN allows the release of cell content. Interestingly, LDH release was prevented significantly in apoptotic cells without AMN by colchicine treatment when caspases were inhibited by z-VAD suggesting that caspase-mediated cleavage of plasma membrane and cellular cortex proteins was essential for releasing cell content.

Previously, it has been demonstrated that caspases cleave and inactivate two key proteins in calcium homeostasis, PMCA-4 and NCX, in cells undergoing apoptosis.[12,13] PMCA-4 and NCX cleavage impairs intracellular Ca^{2+} handling, which results in Ca^{2+} overload and secondary necrosis. To confirm this hypothesis and to demonstrate the protective role of AMN during apoptosis, we measured intracellular calcium levels by FLUO-4 staining. Genuine apoptotic cells with AMN showed a moderate increase of FLUO-4 fluorescence respect to control cells. However, apoptotic cells without AMN by colchicine treatment or cells in secondary necrosis showed a notably increase of FLUO-4 fluorescence suggesting calcium overload (Figure 6b). Interestingly, calcium overload was significantly abolished in apoptotic cells without AMN by colchicine treatment but in
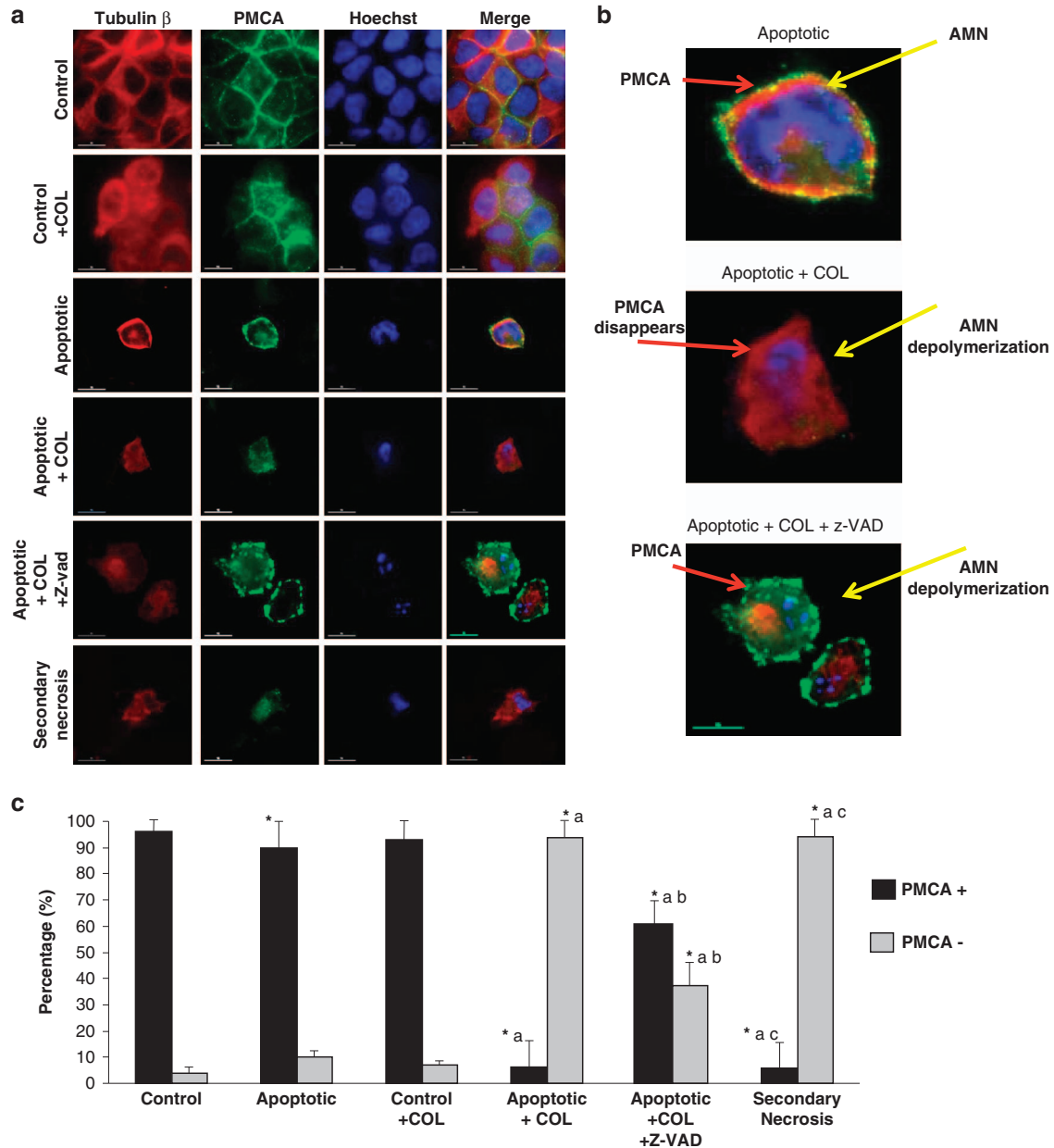
Figure 4 PMCA-4 integrity during the execution phase of apoptosis and after AMN disorganization. (**a**) Fluorescence microscopy of PMCA-4 control cells, control cells treated with 2 μM colchicine (Control + COL) for 1 h, apoptotic cells, apoptotic cells treated with 2 μM colchicine (Apoptotic + COL) for 1 h or colchicine plus 50 μM z-VAD (Apoptotic + COL + z-VAD) for 1 h and secondary necrotic cells. H460 cells were grown on glass coverslips and apoptosis was induced as is described in the enriched apoptotic assay in Materials and Methods. Secondary necrotic cells were collected from the floating cells in de medium after the treatment and cytospined on a slide. Apoptotic cells were treated with colchicine or colchicine plus the pan-caspase inhibitor z-VAD to examine the effect of AMN depolymerization when caspases were active or inhibited. Then, cells were fixed and immunostained with anti-PMCA-4 (green) and anti-β-tubulin (red). Nuclear morphology was revealed by staining with Hoechst 33342. Bar = 15 μm. (**b**) Magnification of apoptotic cells and apoptotic cells after 1 h of treatment with colchicine or colchicine plus z-VAD. (**c**) PMCA positive and negative cells were quantified by microscopic counting. More than 100 cells were examined for each experimental condition. *P<0.01 significant differences with respect to Control cells. [a]P<0.01, significant differences with respect to Apoptotic cells. [b]P<0.01, significant differences with respect to Apoptotic + COL. [c]P<0.01, significant differences with respect to Apoptotic + COL + z-VAD treated cells

which caspases were inhibited by z-VAD, suggesting that the activity of caspases were critical for PMCA-4 and NCX inactivation and subsequent calcium overload typical features of cells undergoing secondary necrosis.

Likewise, cleavage of Na$^+$/K$^+$ pump subunit β may alter sodium extrusion and increase intracellular sodium levels. Apoptotic cells with AMN showed a moderate increase of sodium levels respect to control cells. However, apoptotic cells without AMN by colchicine treatment or cells in secondary necrosis showed a notably increase of sodium levels (Figure 6c). Sodium levels were significantly reduced in apoptotic cells devoid of AMN by colchicine treatment but in which caspases were inhibited by z-VAD, suggesting that the activity of caspases were critical for Na$^+$/K$^+$ pump subunit
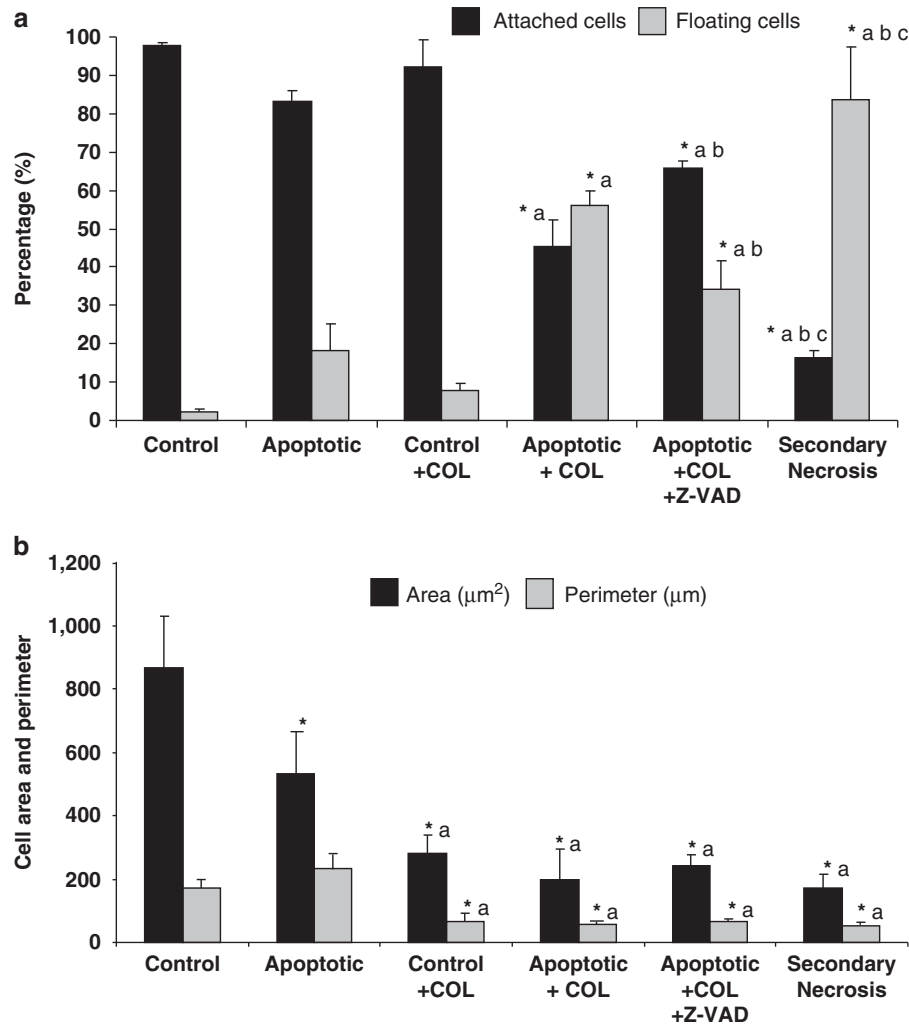
Figure 5 Effect of AMN disorganization in cell area and substrate detachment. (a) Cell area at the maximum cell perimeter was determined by microscopic studies using the Image J software in control cells, control cells treated with 2 μM colchicine (Control + COL), apoptotic cells, apoptotic cells treated with 2 μM colchicine (Apoptotic + COL) for 1 h or colchicine plus 50 μM z-VAD (Apoptotic + COL + z-VAD) for 1 h and secondary necrotic cells. H460 cells were grown on glass coverslips and apoptosis was induced as is described in the enriched apoptotic assay in Materials and Methods. Secondary necrotic cells were collected from the floating cells in de medium after the treatment and cytospined on a slide. Apoptotic cells were treated with colchicine or colchicine plus the pan-caspase inhibitor z-VAD to examine the effect of AMN depolymerization when caspases were active or inhibited. More than 100 cells were examined for each experimental condition. (b) Floating and attached cells were quantified by microscopic counting. Data represent the means ± S.D. of three independent experiments. *$P < 0.01$ significant differences with respect to Control cells. [a]$P < 0.01$, significant differences with respect to apoptotic cells. [b]$P < 0.01$, significant differences with respect to Apoptotic + COL. [c]$P < 0.01$, significant differences with respect to Apoptotic + COL + z-VAD treated cells

β inactivation and subsequent sodium overload typical features of cells undergoing secondary necrosis.

In previous works, we demonstrated that AMN during apoptosis depends on energized mitochondria.[14] As expected, in apoptotic cells with AMN, we found hyperpolarized mitochondria and high ATP levels (Figures 6c and d). On the contrary, when AMN was disorganized by colchicine o in secondary necrotic cells we found mitochondrial depolarization and low ATP levels (Figures 6c and d). Mitochondria depolarization and low ATP levels were prevented significantly in apoptotic cells without AMN by colchicine treatment when caspases were inhibited by z-VAD, suggesting that caspase-mediated cleavage of plasma membrane and cellular cortex proteins in the absent of AMN was important for inducing the bioenergetic collapse in apoptotic cells.

High phosphatidylserine (PS) exposure in apoptotic cells with AMN. Phosphatidylserine (PS) is actively localized on the inner leaflet of the plasma membrane in healthy cells. The asymmetry of its distribution is lost in apoptotic cells. To examine the role of AMN in PS exposure, we analyzed the binding of annexin V-FITC to PS by immunofluorescence and flow cytometry analysis in control, apoptotic and secondary necrotic cells. Apoptotic cells were also treated with colchicine or colchicine plus the pan-caspase inhibitor z-VAD for 1 h to examine the effect of AMN depolymerization when caspases were active or inhibited. Figures 7a, b and c show clearly that PS was highly translocated in apoptotic cells with AMN. However, PS translocation was significantly reduced in apoptotic cells without AMN by colchicine treatment or cells in secondary
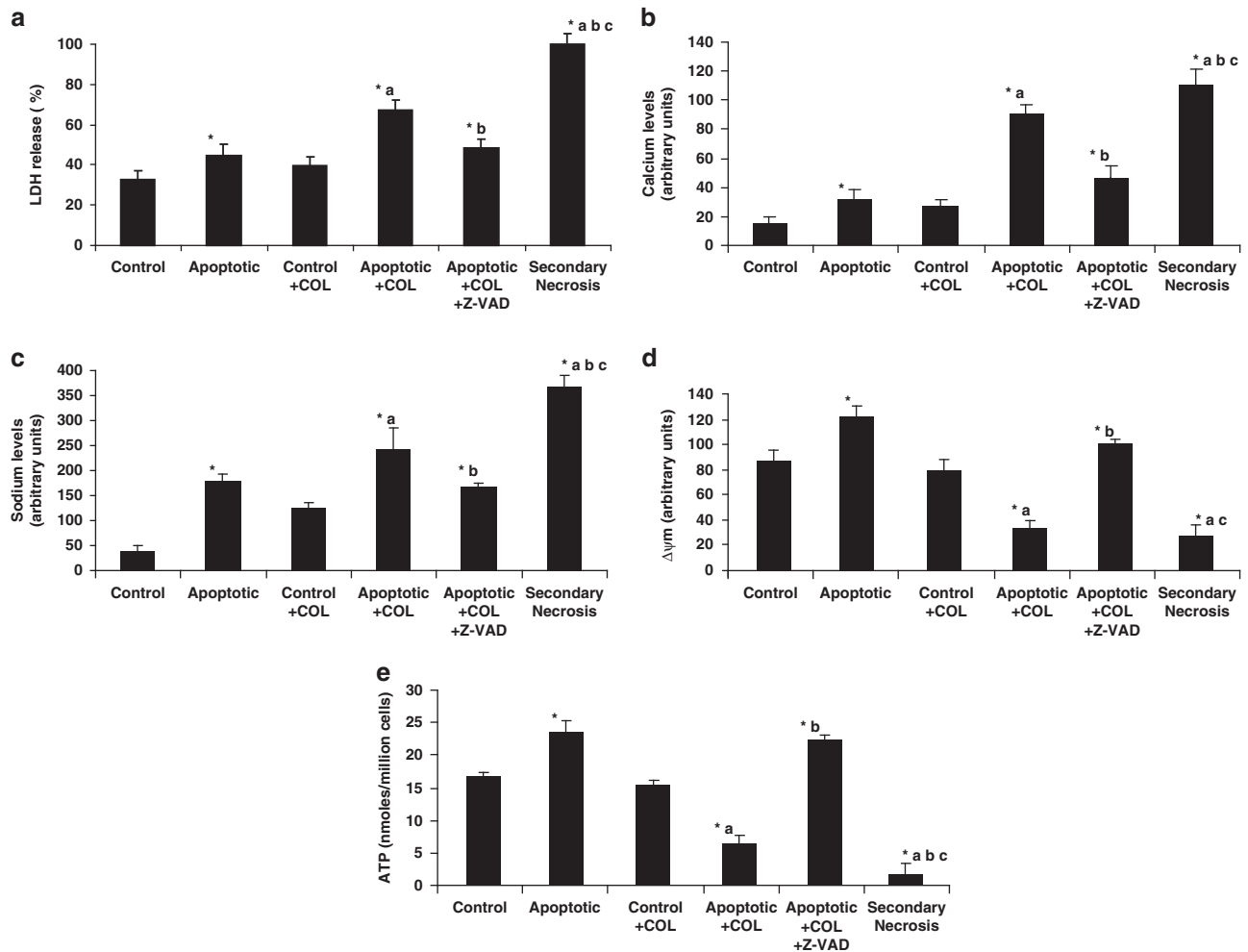
Figure 6 Effect of microtubule disorganization on LDH release, intracellular calcium and sodium levels, mitochondrial membrane potential and ATP levels in apoptotic cells. LDH release, calcium and sodium levels, mitochondrial membrane potential and ATP levels were measured in control cells, control cells treated with 2 μM colchicine (Control + COL), apoptotic cells with AMN (Apoptotic), apoptotic cells treated with 2 μM colchicine (Apoptotic + COL) for 1 h or colchicine plus 50 μM z-VAD (Apoptotic + COL + z-VAD) for 1 h and secondary necrotic cells. H460 cells were grown on glass coverslips and apoptosis was induced as is described in the enriched apoptotic assay in Material and Methods. Apoptosis was induced as is described in the enriched apoptotic assay in Materials and Methods. Secondary necrotic cells were collected from the floating cells in de medium after the treatment. Apoptotic cells were treated with colchicine or colchicine plus the pan-caspase inhibitor z-VAD to examine the effect of AMN depolymerization when caspases were active or inhibited. (**a**) After treatments, LDH release in fresh medium for 1 h was measured as is described in Material and Methods. (**b**) Intracellular calcium levels were measured by flow cytometry using the calcium indicator FLUO-4 (1 μM). (**c**) Intracellular sodium levels were measured by flow cytometry using the sodium indicator SBFI-AM (5 μM). (**d**) Mitochondrial membrane potential ($\Delta\Psi$m) was determined by MitoTracker Red staining and flow cytometry analysis as is described in Material and Methods. (**e**) ATP levels were determined by luminescence as is described in Material and Methods. *$P < 0.01$ significant differences with respect to Control cells. [a]$P < 0.01$, significant differences with respect to Apoptotic cells. [b]$P < 0.01$, significant differences with respect to Apoptotic + COL. [c]$P < 0.01$, significant differences with respect to Apoptotic + COL + z-VAD treated cells

necrosis. High levels of PS externalization were significantly recovered in apoptotic cells without AMN by colchicine treatment when caspases were inhibited by z-VAD, suggesting that caspase-mediated cleavage of plasma membrane and cellular cortex proteins also impairs PS externalization. These results suggest that proper PS externalization also depends on the presence of AMN.

AMN in apoptotic cells enhances interactions with macrophages. As the presence of AMN in apoptotic cells effectively increase cell surface area and allows high PS externalization, we tested their influence upon binding and uptake by phagocytes. In the absence of AMN by colchicine treatment or in secondary necrotic cells, that is associated

with low PS externalization, the proportion of macrophages interacting with and engulfing apoptotic cells was markedly reduced compared with apoptotic cells with AMN and high PS externalization (Figures 8a and b). However, the proportion of macrophages interaction/engulfing with apoptotic cells was restored in apoptotic cells without AMN by colchicine treatment when caspases were inhibited by z-VAD that also was associated with high PS externalization.

Discussion

In the present study, we show new data demonstrating that AMN indeed works as physical barrier impeding active caspases to reach and cleave critical proteins in the cellular
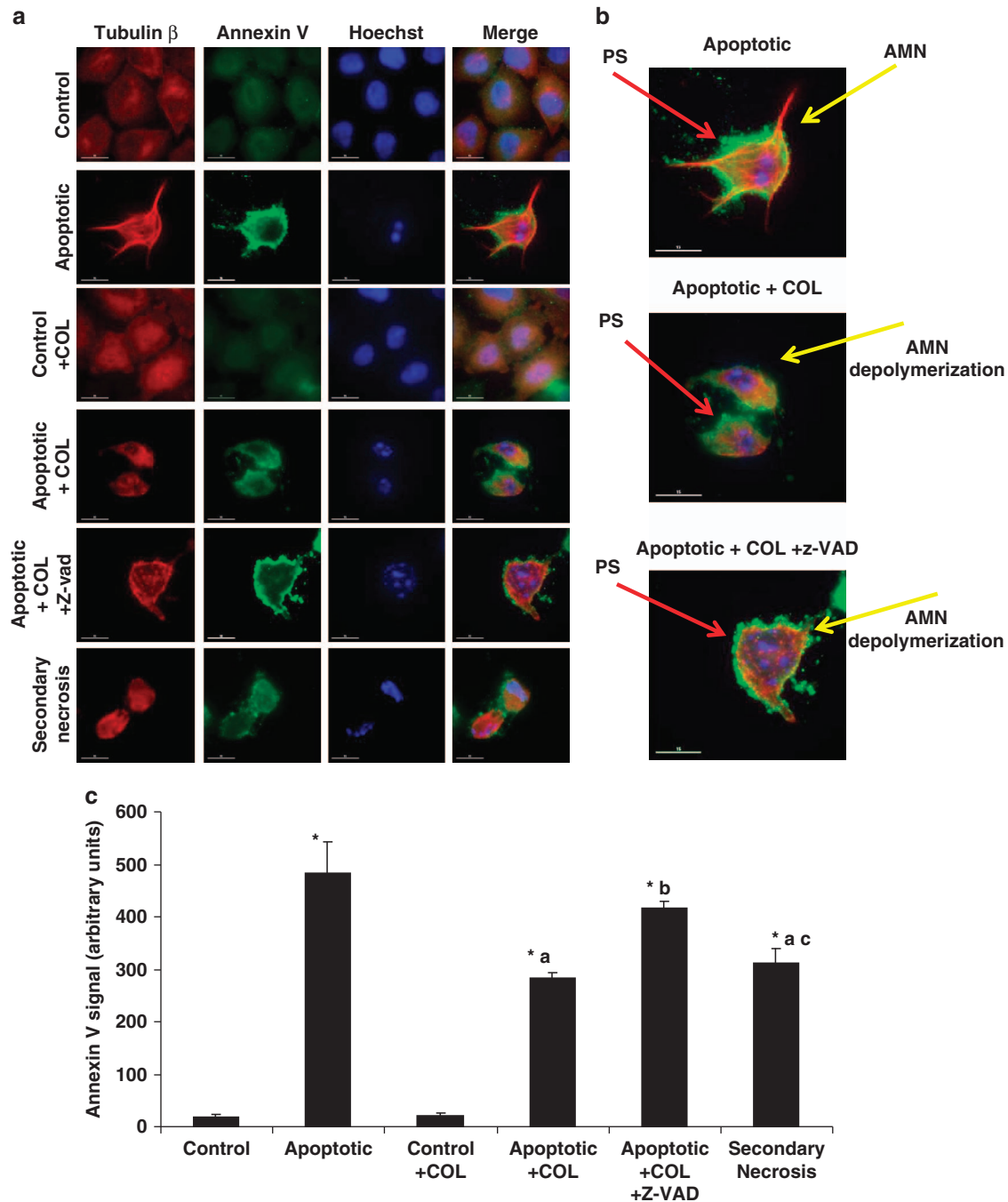
Figure 7 Effect of apoptotic microtubules on PS externalization. (**a**) Fluorescence microscopy of microtubules and PS externalization in control cells, control cell treated with colchicine for 1 h (Control + COL), apoptotic cells with AMN (Apoptotic), apoptotic cells treated with 2 μM colchicine (Apoptotic + COL) for 1 h or colchicine plus 50 μM z-VAD (Apoptotic + COL + z-VAD) for 1 h and secondary necrotic cells. H460 cells were grown on glass coverslips and apoptosis was induced as is described in the enriched apoptotic assay in Materials and Methods. Secondary necrotic cells were collected from the floating cells in de medium after treatment and cytospined onto a slide. Apoptotic cells were treated with colchicine or colchicine plus the pan-caspase inhibitor z-VAD to examine the effect of AMN depolymerization when caspases were active or inhibited. Then, cells were fixed and immunostained with anti-β-tubulin (red), and PS externalization was revealed by staining with Annexin V-FITC. Nuclear morphology was revealed by staining with Hoechst 33342 (1 μg/ml). Bar = 15 μm). (**b**) Magnification of apoptotic cells and apoptotic cells after 1 h of treatment with colchicine or colchicine plus z-VAD. (**c**) PS externalization was quantified by flow cytometry as described in Material and Methods. Data represent the means ± S.D. of three independent experiments. *$P < 0.01$ significant differences with respect to Control cells. [a]$P < 0.01$, significant differences with respect to Apoptotic cells. [b]$P < 0.01$, significant differences with respect to Apoptotic + COL. [c]$P < 0.01$, significant differences with respect to Apoptotic + COL + z-VAD treated cells

cortex and plasma membrane proteins to preserve plasma membrane integrity. We found that the AMN was present in all genuinely apoptotic cells but was disrupted in cells undergoing secondary necrosis. Furthermore, AMN disorganization in apoptotic cells by a short incubation with colchicine allowed caspase-mediated cleavage of cell cortex and plasma
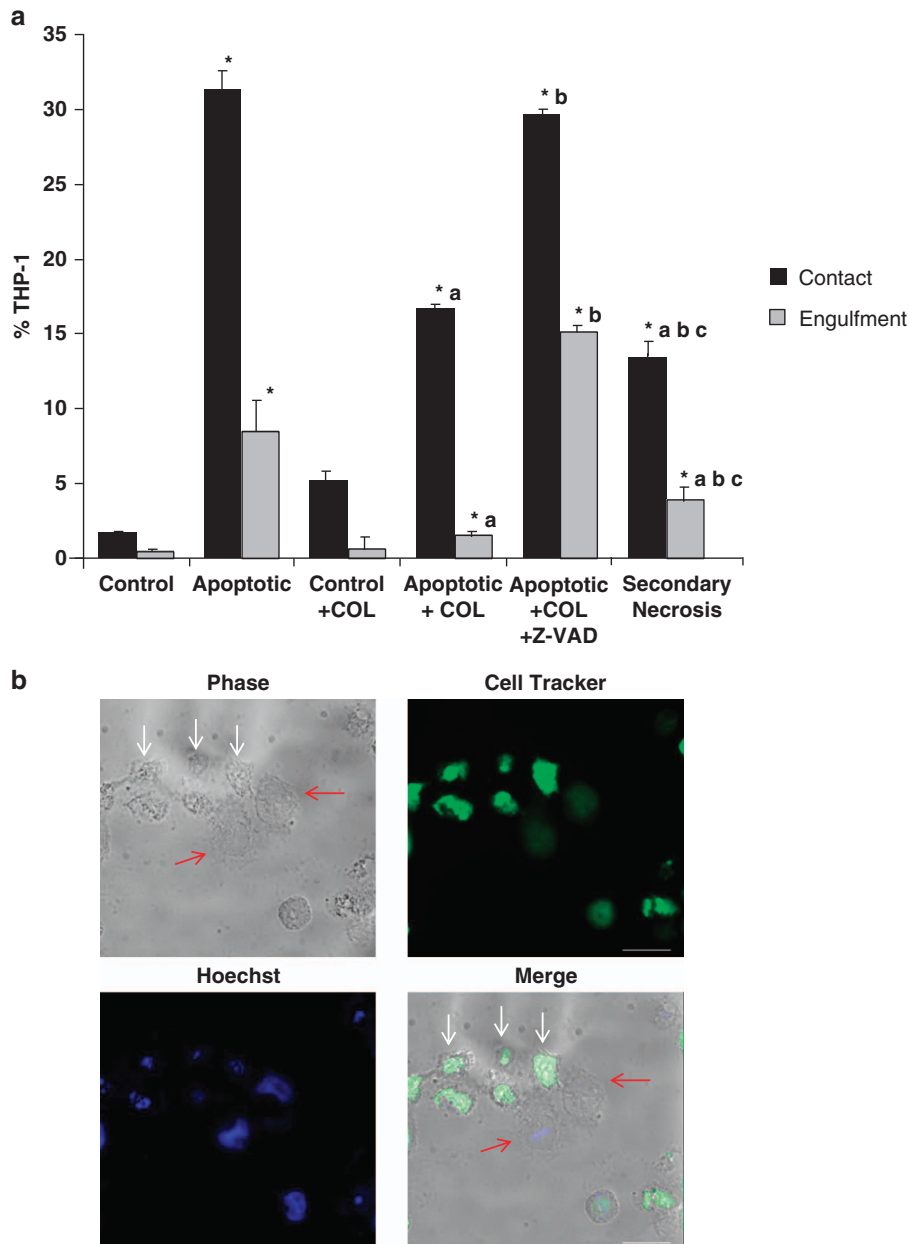
Figure 8 Phagocytosis assay: Interaction between apoptotic cells and phagocytes. (**a**) Proportion of THP-1 macrophages interacting and engulfing apoptotic H460 cells. CellTrackerTM Green-labelled H460 cells were induced into apoptosis by CPT/cytochalasin as described in Materials and Methods. Secondary necrotic cells were collected from the floating cells in the medium after treatment and cytospined onto a slide. Apoptotic cells were then incubated for 1 h in the absence or presence of 2 μM colchicine for AMN depolimerization (Apoptotic + COL) or colchicine plus 50 μM z-VAD to examine the effect of AMN depolymerization when caspases were inhibited (Apoptotic + COL + z-VAD). Cells under the different experimental conditions were then co-incubated with THP-1 macrophages. Nuclear morphology was revealed by staining with Hoechst 33342 (1 μg/ml). Data represent the means ± S.D. of three independent experiments. *$P < 0.01$ significant differences with respect to Control cells. [a]$P < 0.01$, significant differences with respect to Apoptotic cells. [b]$P < 0.01$, significant differences with respect to Apoptotic + COL. [c]$P < 0.01$, significant differences with respect to Apoptotic + COL + z-VAD treated cells. (**b**) Wide-field images of CellTracker Green-labelled apoptotic H460 cells (white arrows) interacting with THP-1 macrophages (red arrows). Bars = 25 μm

membrane proteins such as, α-spectrin, paxilin, FAK, E-cadherin, PMCA-4, NCX, integrin β4 and Na$^+$/K$^+$ pump subunit β. These events were associated with increase cell permeability, calcium and sodium overload and bioenergetics failure, which could in turn accelerate secondary necrosis by inducing ionic imbalance and cellular collapse.[13] The critical role of caspase-mediated cleavage of cortical and plasma

membrane proteins after AMN disorganization was demonstrated because the concomitant addition of colchicine and Z-VAD blocked protein cleavage and significantly prevented plasma membrane permeability, cell detachment, LDH release, calcium and sodium overload and bioenergetics failure.

The significance of membrane-cytoskeleton network in maintaining plasma membrane integrity has been

demonstrated in erythrocytes, in which deficiencies or defects in the cytoskeletal proteins spectrin or spectrin-associated proteins are associated with increased fragility and lysis of the plasma membrane.[15] Changes in the cytoskeletal network beneath the plasma membrane (as α-spectrin cleavage by caspases after AMN depolimerization) may contribute to increase in membrane permeability during cell injury/death.

Focal adhesions are large, dynamic protein complexes through which the cytoskeleton of a cell connects to the extracellular matrix.[16] When cells adhere to the extracellular matrix, integrin receptors initiate signals to cluster more integrins together and to recruit cytoskeleton proteins, adapters (such as paxillin,) and kinases (such as FAK) to their cytoplasmic tails, forming a 'focal adhesion complex'.[17,18,19] Focal adhesions provide not only mechanical support to the cells but also signals necessary anchorage-dependent cellular responses.[20,21] Hydrolysis of 'focal adhesion complex' proteins by caspases after AMN depolymerization could break the membrane-cytoskeleton linkage and decrease the physical support leading to cell detachment. In this study, we show that FAK, integrin $\beta4$ and paxilin are cleaved in apoptotic cells when AMN was disorganized by colchicine treatment or in secondary necrotic cells without AMN.

We have also demonstrated that E-cadherins are cellular cortex proteins targeted by caspases when AMN is depolymerized. Cadherins are transmembrane glycoproteins involved in cell-cell adherence.[22] Previously, it has been showed that cadherins are also targeted during apoptosis.[23,24,25] According to our observations, caspase-mediated cleavage of E-cadherins and the loss of cell-cell contacts are likely to represent an important process during the extrusion of apoptotic cells.

The Na^+/K^+-ATPase (Na^+/K^+-pump) acts as an electrogenic ion transporter in the plasma membrane of all mammalian cells.[26] Failure of the Na^+/K^+-pump results in depletion of intracellular K^+, accumulation of intracellular Na^+, and, consequently, leads to membrane depolarization.[27] The Na^+-K^+-ATPase is composed of two subunits. The α-subunit is the action subunit of the pair; it binds ATP and both sodium and potassium ions, and contains the phosphorylation site.[28] The smaller β-subunit is absolutely necessary for activity of the complex. In our work we found that Na^+/K^+-ATPase β-subunits, but not α-subunits, were cleaved by caspases after AMN depolymerization, which may contribute to ionic imbalance and increase plasma membrane permeability. Consistent with this hypothesis, we found that sodium levels were notably increased after AMN depolymerization by colchicine and partially restored when AMN was disorganized but caspases were blocked by z-VAD.

Changes in cytosolic calcium has a critical role in apoptosis by triggering the activation of Ca^{2+}-dependent events thereby inducing global intracellular and morphological modifications.[29] Among these changes, an early redistribution of plasma membrane PS is a typical feature of cells undergoing apoptosis.[30,31] The resulting presence of PS within the outer plasma membrane may serve as a recognition signal for phagocytosis.[32,33] Previously, we demonstrated that calcium levels were moderately increased in apoptotic cells with AMN.[10] However, AMN disruption by colchicine allows the caspase-mediated cleavage of key proteins involved in

calcium extrusion such as PMCA-4 and NCX, and consequently calcium overload. PMCAs are vital caspase substrates for the subroutine of the death program leading to secondary necrosis. Cells expressing PMCA-4 mutants that lack the caspase cleavage site(s) prevents calcium overload during apoptosis and markedly delays secondary necrosis.[13] Moreover, NCX drives calcium efflux in addition to PMCAs.[34] NCX has a low calcium affinity, but high calcium transporting velocity, which is required to rapidly eject large amounts of calcium.[35] Our results show that both calcium pumps and exchangers are cleaved by caspases when AMN is depolymerized by colchicine treatment, suggesting that inactivation of plasma membrane calcium transporters is a relevant process leading apoptotic cells to secondary necrosis. Calcium overload can induce: (1) activation of calpains, leading to more extensive disruption of cytoskeleton components, (2) activation of calcium-dependent phospholipases, and disruption of membrane permeability, (3) Mitochondrial permeabilization and bioenergetics collapse.[36,37]

Apoptosis requires energy, because it is a highly regulated process involving a number of ATP-dependent steps.[38,39,40] Moreover, depletion of cellular ATP was found to cause switching of the form of cell death, from apoptotic cell death triggered by a variety of stimuli to necrotic cell death.[41,42] Our new results suggest that AMN disorganization and the consequent caspase-dependent inactivation of plasma membrane calcium and sodium pumps induces calcium and sodium overload that it has been reported to induce mitochondria depolarization and cessation of ATP synthesis.[36,37]

The efficient phagocytosis of apoptotic cells by macrophages reduces the potential for an inflammatory response by ensuring that the dying cells are cleared before their intracellular contents are released.[43,44] Early apoptotic cells are targeted for phagocytosis through the externalization of PS.[45] PS exposure has been reported to be a caspase and energy dependent process,[39,46] but its mechanism has not been totally elucidated. A combined effect of downregulation of a phospholipid translocase activity and activation of a lipid scramblase may contribute to PS exposure.[47] Consistent with a role of AMN for proper PS exposure, we found that the phagocytosis of apoptotic cells with AMN coincided with high PS externalization while it was reduced when AMN was absent and PS externalization was low.

In summary, we propose a model (Supplementary Figure S3) where the AMN works as a physical barrier preventing caspases to reach the cellular cortex and the cleavage of essential proteins involved in plasma membrane integrity that allows correct ionic homeostasis, bioenergetics status and high PS externalization for efficient clearance by macrophages.

Materials and Methods

Reagents. Camptothecin (CPT) was purchased from Alexis Corporation (Nottingham, East Midlands, UK). Cytochalasin, colchicine, Phalloidin-coumarin, trypsin, anti-ROCK-1, anti-actin and anti-α-tubulin, were purchased from Sigma Chemical Co (Sigma, St. Louis, MO, USA). Anti-β-tubulin antibodies were from Chemicon International (Temecula, CA, USA). Hoechst 33342, FITC-labeled goat anti-mouse and tetramethyl rhodamine goat anti-rabbit antibodies, Dead Red reagent, SBFI-AM (Na^+), FLUO-4 were purchased from Molecular Probes (Eugene, OR, USA). Anti-active caspase-3, anti-active caspase-7, anti-caspase-9 and anti-cleaved PARP were obtained from Cell Signaling Technology (Beverly, MA, USA). Anti-lamin B, anti-Cytokeratin 5/8, anti-cytokeratin 18, anti-FAK,

anti-PMCA-4, anti-α-spectrin, anti-NCX, anti-paxilin, anti-integrin $\beta 4$, anti-Na$^+$/K$^+$ pump subunit β and anti-Na$^+$/K$^+$ pump subunit α were purchased from Santa Cruz Biotecnology (Santa Cruz, CA, USA). Anti-E-cadherin was purchased from BD Biosciences Pharmingen (San Jose, CA, USA). Anti-GADPH was purchased from Calbiochem Merck Millipore (Darmstadt, Germany). z-VAD was purchased from RD-System (Minneapolis, MN, USA).

Cell culture. Non-small lung cancer cell line, H460 was a gift from Dr. PJ Woll (CRC Department of Clinical Oncology, City Hospital, Nottingham, UK). Cells were cultured in RPMI medium supplemented with penicillin, streptomycin and 10% fetal bovine serum at 37 °C.

Enriched apoptotic assay. Cells were induced into apoptosis by treatment with 10 μM CPT, an anticancer drug which inhibits the DNA enzyme topoisomerase I. To increase the proportion of attached apoptotic cells with AMN formation. H460 cells were treated with CPT + cytochalasin (2 μM) for 48 h. To prevent cell cycle effects, cytochalasin was added 24 h after CPT treatment. Inhibiting actin polymerization and consequently actin contraction with cytochalasin, CPT induced apoptosis but apoptotic cells maintained the spread state and remained attached to the flask or slide.[48] For AMN depolymerization, enriched apoptotic cells were incubated with 2 μM colchicine (COL) or colchicine plus z-VAD (50 μM) to prevent caspase-mediated cleavage after AMN disorganization. Secondary necrotic cells were collected from the floating cells in de medium after the treatment.

Analysis of apoptosis. Apoptosis was defined by the occurrence of cells with nuclear condensation and fragmentation by Hoechst staining, but retaining plasma membrane integrity (measured by exclusion of the membrane-imperme-able dye, Dead Red reagent). Apoptosis was also assessed by caspase activation, cytochrome c release, lack of actin cytoskeleton, presence of apoptotic microtubules and/or cell morphology by phase-contrast microscopy. Primary necrosis was defined as loss of plasma membrane integrity without signs of nuclear condensation or fragmentation. Secondary necrosis was determined by scoring over time apoptotic cells, which became permeable to the Dead Red reagent. Cells were counted for up to 48 h after CPT/cytochalasin-exposure. At this time, the proportion of primary necrotic cells did not exceed 1% and was identical in both control and treated cells (data not shown). In each case 10 random fields and more of 100 cells were counted. To differentiate between genuine apoptotic cells and cells in secondary necrosis Dead Red reagent was added to the cells 10 min before fixation.

Immunofluorescence studies. H460 cells were grown on 1mm (Goldseal No. 1) glass coverslips for 24–48 h in RPMI containing 10% fetal bovine serum. After treatments, cells were rinsed once with PBS, fixed in 3.8% paraformaldehyde for 5 min at room temperature, and permeabilized in 0.1% saponin for 5 min. For immunostaining, glass coverslips were incubated with primary antibodies diluted 1 : 100 in PBS for 1–2 h at 37 °C in a humidified chamber. Excess antibody binding was removed by washing the coverslips with PBS (three times, 5 min). The secondary antibody, a FITC-labeled goat anti-mouse antibody or a tetramethyl rhodamine goat anti-rabbit (Molecular Probes), diluted 1 : 100 in PBS, were added and incubated for 1 h 37 °C. Coverslips were then rinsed with PBS for 3 min, incubated for 1 min with PBS containing Hoechst 33342 (1 μg/ml) and washed with PBS (three 5 min washes). Finally, the coverslips were mounted onto microscope slides using Vectashield Mounting Medium (Vector Laboratories, Burlingame, CA, USA) and analyzed using an upright fluorescence microscope (Leica DMRE, Leica Microsystems GmbH, Wetzlar, Germany). Deconvolution studies and 3D projections were performed using a DeltaVision system (Applied Precision, Issaquah, WA, USA) with an Olympus IX-71 microscope with × 100 objective/1.35 NA and × 60 objective/1.40 NA (Olympus, Shinjuku, Tokyo, Japan) and filters set for DAPI, fluorescein isothiocyanate and rhodamine provided by Applied Precision. Acquired z planes were separated by 0.3 μm, and an average of 50 planes was taken for each nucleus. The 3D stacks were deconvolved using the Softworx software algorithm (conservative ratio method, 10 iterations; Applied Precision).

Western blotting analysis. Whole-cellular lysates were prepared in a buffer, gentle shaking, composed of 0.9% NaCl, 20 mM Tris-ClH, pH 7.6, 0.1% triton X-100, 1 mM phenylmethylsulfonylfluoride and 0.01% leupeptine. Electro-phoresis was carried out in a 10–15% acrylamide SDS-polyacrylamide gel electrophoresis. Proteins were transferred to Immobilon membranes (Amersham Pharmacia, Buckinghamshire, UK). Specific antibodies were used to detect

proteins by western blotting. Proteins were electrophoresed, transferred to nitrocellulose membranes, and after blocking over night at 4 °C, incubated with the respective antibody solution at 1 : 1000 dilutions. Then, membranes were probed with their respective secondary antibody (1 : 2500). Immunolabeled proteins were detected by using a chemioluminiscence method (Bio-Rad, Hercules, CA, USA). Protein was determined by the Bradford method.[49]

Cell content release: LDH determination. Plasma membrane integrity and cell content release was monitored by measuring LDH activity into the incubation medium. This was done using a commercial kit (CytoTox 96 Non-Radioactive Cytotoxicity Assay from Promega (Madison, WI, USA).

Determination of intracellular calcium levels by flow cytometry. H460 cells were incubated for 60 min at 37 °C in medium supplemented with 1 μM FLUO-4, AM. Cells were then washed three times with RPMI medium, fixed with 3.8% paraformaldehyde, and analyzed by flow cytometry using an EPICS Elite flow cytometer (Beckman-Coulter, Hialeah, FL, USA).

Determination of intracellular sodium levels by flow cytometry. For intracellular sodium measurements, 2 μl of 2.5 mM SBFI-AM (Na +) stock (in Me$_2$SO) were added to 1 ml of cells (5–10 × 10^5 cells/ml), yielding a final concentration of 5 μM. The dye was loaded into the cells for 1 h at 37 °C, 7% CO$_2$ atmosphere before the time of examination by flow cytometry.

Measurement of mitochondrial membrane potential ($\Delta\psi$m) by flow cytometry. H460 cells were incubated for 60 min at 37 °C in medium supplemented with 1 μm Mitotracker Red. Cells were then washed three times with RPMI medium, fixed with 3.8% paraformaldehyde, and analyzed by flow cytometry.

Determination of intracellular ATP levels. ATP was determined luminometrically. ATP levels were determined by using a luciferase-based assay, according to Molecular Probes's directions, using a Tuner Designs Luminometer TD 20/20 (Sunnyvale, CA, USA).

Determination of PS externalization. PS translocation from the inner to the outer leaflet of the plasma membrane is one of the earliest apoptotic features. We used the PS-binding protein annexin-V conjugated with FITC to identify PS exposure in H460 cells. The binding of annexin-V to cell surface PS was detected with a commercial Annexin Apoptosis Kit (Santa Cruz Biotechnology, Santa Cruz, CA, USA) according to the manufacturer's instructions. To distinguish cells that had lost membrane integrity, propidium iodide (PI) was added to a final concentration of 10 μg/ml immediately before analysis. Apoptotic cells were identified either by fluorescence microscopy or by flow cytometry. Hoechst 33342 (1 μg/ml) staining was used to reveal nuclear condensation/fragmentation.

Phagocytosis assays. CellTracker-labelled H460 cells adhered to glass coverslips were induced into apoptosis by CPT/cytochalasin treatment and then were incubated for 1 h in the absence or presence of colchicine or colchicine plus z-VAD. Then, cells were washed and coincubated with PMA-differentiated THP-1 macrophages (150,000 cells/well). Floating apoptotic cells representing secondary necrotic cells were cytospined onto coverslips and also coincubated with PMA-differentiated THP-1 macrophages. After 8 h of coincubation at 37 °C, coverslips were washed extensively in PBS, and cells fixed in 3.8% paraformaldehyde. The number of THP-1 macrophages interacting (bound and engulfed) and engulfing cell fragments was calculated in 10 random fields in triplicate by fluorescence and phase-contrast microscopy.

Statistical analysis. All results are expressed as means ± S.D. unless stated otherwise. Two-tail Student's *t*-tests (paired and unpaired, according to samples) or ANOVA variance analysis were used as appropriate for statistical analysis. Only *P*–values < 0.05 were considered as statistically significant.

Conflict of Interest

The authors declare no conflict of interest.

1. Kerr JF, Wyllie AH, Currie AR. Apoptosis: a basic biological phenomenon with wide-ranging implications in tissue kinetics. *Br J Cancer* 1972; **26**: 239–257.
2. Savill J, Dransfield I, Gregory C, Haslett C. A blast from the past: clearance of apoptotic cells regulates immune responses. *Nat Rev Immunol* 2002; **2**: 965–975.
3. Zong WX, Thompson CB. Necrotic death as a cell fate. *Genes Dev* 2006; **20**: 1–15.
4. Afford S, Randhawa S. Demystified Apoptosis. *Mol Pathol* 2000; **53**: 55–63.
5. Mills JC, Stone NL, Pittman RN. Extranuclear apoptosis. The role of the cytoplasm in the execution phase. *J Cell Biol* 1999; **146**: 703–708.
6. Pittman S, Geyp M, Fraser M, Ellem K, Peaston A, Ireland C. Multiple centrosomal microtubule organising centres and increased microtubule stability are early features of VP-16-induced apoptosis in CCRF-CEM cells. *Leuk Res* 1997; **21**: 491–499.
7. Pittman SM, Strickland D, Ireland CM. Polymerization of tubulin in apoptotic cells is not cell cycle dependent. *Exp Cell Res* 1994; **215**: 263–272.
8. Moss DK, Betin VM, Malesinski SD, Lane JD. A novel role for microtubules in apoptotic chromatin dynamics and cellular fragmentation. *J Cell Sci* 2006; **119**(Pt 11): 2362–2374.
9. Moss DK, Lane JD. Microtubules: forgotten players in the apoptotic execution phase. *Trends Cell Biol* 2006; **16**: 330–338.
10. Sanchez-Alcazar JA, Rodriguez-Hernandez A, Cordero MD, Fernandez-Ayala DJ, Brea-Calvo G, Garcia K *et al.* The apoptotic microtubule network preserves plasma membrane integrity during the execution phase of apoptosis. *Apoptosis* 2007; **12**: 1195–1208.
11. Sanchez-Alcazar JA, Khodjakov A, Schneider E. Anticancer drugs induce increased mitochondrial cytochrome c expression that precedes cell death. *Cancer Res* 2001; **61**: 1038–1044.
12. Bano D, Munarriz E, Chen HL, Ziviani E, Lippi G, Young KW *et al.* The plasma membrane Na + /Ca2 + exchanger is cleaved by distinct protease families in neuronal cell death. *Ann N Y Acad Sci* 2007; **1099**: 451–455.
13. Schwab BL, Guerini D, Didszun C, Bano D, Ferrando-May E, Fava E *et al.* Cleavage of plasma membrane calcium pumps by caspases: a link between apoptosis and necrosis. *Cell Death Differ* 2002; **9**: 818–831.
14. Oropesa M, de la Mata M, Maraver JG, Cordero MD, Cotan D, Rodriguez-Hernandez A *et al.* Apoptotic microtubule network organization and maintenance depend on high cellular ATP levels and energized mitochondria. *Apoptosis* 2011; **16**: 404–424.
15. Palek J, Sahr KE. Mutations of the red blood cell membrane proteins: from clinical evaluation to detection of the underlying genetic defect. *Blood* 1992; **80**: 308–330.
16. Chen CS, Alonso JL, Ostuni E, Whitesides GM, Ingber DE. Cell shape provides global control of focal adhesion assembly. *Biochem Biophys Res Commun* 2003; **307**: 355–361.
17. Critchley DR. Focal adhesions—the cytoskeletal connection. *Curr Opin Cell Biol* 2000; **12**: 133–139.
18. Gilmore AP, Burridge K. Molecular mechanisms for focal adhesion assembly through regulation of protein-protein interactions. *Structure* 1996; **4**: 647–651.
19. Miyamoto S, Katz BZ, Lafrenie RM, Yamada KM. Fibronectin and integrins in cell adhesion, signaling, and morphogenesis. *Ann N Y Acad Sci* 1998; **857**: 119–129.
20. Clark EA, Brugge JS. Integrins and signal transduction pathways: the road taken. *Science* 1995; **268**: 233–239.
21. Giancotti FG, Ruoslahti E. Integrin signaling. *Science* 1999; **285**: 1028–1032.
22. Fouquet S, Lugo-Martinez VH, Chambaz J, Cardot P, Pincon-Raymond M, Thenet S. [Control of the survival/apoptosis balance by E-cadherin: role in enterocyte anoikis]. *J Soc Biol* 2004; **198**: 379–383.
23. Herren B, Levkau B, Raines EW, Ross R. Cleavage of beta-catenin and plakoglobin and shedding of VE-cadherin during endothelial apoptosis: evidence for a role for caspases and metalloproteinases. *Mol Biol Cell* 1998; **9**: 1589–1601.
24. Schmeiser K, Grand RJ. The fate of E- and P-cadherin during the early stages of apoptosis. *Cell Death Differ* 1999; **6**: 377–386.
25. Steinhusen U, Weiske J, Badock V, Tauber R, Bommert K, Huber O. Cleavage and shedding of E-cadherin after induction of apoptosis. *J Biol Chem* 2001; **276**: 4972–4980.
26. Rakowski RF, Gadsby DC, De Weer P. Stoichiometry and voltage dependence of the sodium pump in voltage-clamped, internally dialyzed squid giant axon. *J Gen Physiol* 1989; **93**: 903–941.
27. Xiao AY, Wei L, Xia S, Rothman S, Yu SP. Ionic mechanism of ouabain-induced concurrent apoptosis and necrosis in individual cultured cortical neurons. *J Neurosci* 2002; **22**: 1350–1362.
28. Jorgensen PL, Hakansson KO, Karlish SJ. Structure and mechanism of Na,K-ATPase: functional sites and their interactions. *Annu Rev Physiol* 2003; **65**: 817–849.
29. Nicotera P, Orrenius S. The role of calcium in apoptosis. *Cell calcium* 1998; **23**: 173–180.
30. Martin S, Reutelsperger C, McGahon A, Rader J, van Schie R, LaFace D *et al.* Early redistribution of plasma membrane phosphatidylserine is a general feature of apoptosis regardless of the initiating stimulus: inhibition by overexpression of Bcl-2 and Abl 10.1084/jem.182.5.1545.. *J Exp Med* 1995; **182**: 1545–1556.
31. Fadok V, Voelker D, Campbell P, Cohen J, Bratton D, Henson P. Exposure of phosphatidylserine on the surface of apoptotic lymphocytes triggers specific recognition and removal by macrophages. *J Immunol* 1992; **148**: 2207–2216.
32. Fadok VA, Bratton DL, Rose DM, Pearson A, Ezekewitz RAB, Henson PM. A receptor for phosphatidylserine-specific clearance of apoptotic cells.. *Nature* 2000; **405**: 85–90.
33. Verhoven B, Schlegel R, Williamson P. Mechanisms of phosphatidylserine exposure, a phagocyte recognition signal, on apoptotic T lymphocytes. *J Exp Med* 1995; **182**: 1597–1601.
34. Carafoli E, Santella L, Branca D, Brini M. Generation, control, and processing of cellular calcium signals. *Crit Rev Biochem Mol Biol* 2001; **36**: 107–260.
35. Linck B, Qiu Z, He Z, Tong Q, Hilgemann DW, Philipson KD. Functional comparison of the three isoforms of the Na + /Ca2 + exchanger (NCX1, NCX2, NCX3). *Am J Physiol* 1998; **274**(2 Pt 1): C415–C423.
36. Orrenius S, Nicotera P, Zhivotovsky B. Cell death mechanisms and their implications in toxicology. *Toxicol Sci* 2011; **119**: 3–19.
37. Zhivotovsky B, Orrenius S. Calcium and cell death mechanisms: a perspective from the cell death community. *Cell calcium* 2011; **50**: 211–221.
38. Leist M, Single B, Castoldi AF, Kuhnle S, Nicotera P. Intracellular adenosine triphosphate (ATP) concentration: a switch in the decision between apoptosis and necrosis. *J Exp Med* 1997; **185**: 1481–1486.
39. Nicotera P, Leist M, Ferrando-May E. Intracellular ATP, a switch in the decision between apoptosis and necrosis. *Toxicol Lett* 1998; **102-103**: 139–142.
40. Richter C, Schweizer M, Cossarizza A, Franceschi C. Control of apoptosis by the cellular ATP level. *FEBS Lett* 1996; **378**: 107–110.
41. Eguchi Y, Shimizu S, Tsujimoto Y. Intracellular ATP levels determine cell death fate by apoptosis or necrosis. *Cancer Res* 1997; **57**: 1835–1840.
42. Leist M, Single B, Naumann H, Fava E, Simon B, Kuhnle S *et al.* Inhibition of mitochondrial ATP generation by nitric oxide switches apoptosis to necrosis. *Exp Cell Res* 1999; **249**: 396–403.
43. Savill J, Fadok V. Corpse clearance defines the meaning of cell death. *Nature* 2000; **407**: 784–788.
44. Voll RE, Herrmann M, Roth EA, Stach C, Kalden JR, Girkontaite I. Immunosuppressive effects of apoptotic cells. *Nature* 1997; **390**: 350–351.
45. Fadok VA, Bratton DL, Frasch SC, Warner ML, Henson PM. The role of phosphatidylserine in recognition of apoptotic cells by phagocytes. *Cell Death Differ* 1998; **5**: 551–562.
46. Castedo M, Hirsch T, Susin SA, Zamzami N, Marchetti P, Macho A *et al.* Sequential acquisition of mitochondrial and plasma membrane alterations during early lymphocyte apoptosis. *J Immunol* 1996; **157**: 512–521.
47. Moreira ME, Barcinski MA. Apoptotic cell and phagocyte interplay: recognition and consequences in different cell systems. *An Acad Bras Cienc* 2004; **76**: 93–115.
48. Huot J, Houle F, Rousseau S, Deschesnes RG, Shah GM, Landry J. SAPK2/p38-dependent F-actin reorganization regulates early membrane blebbing during stress-induced apoptosis. *J Cell Biol* 1998; **143**: 1361–1373.
49. Bradford MM. A rapid and sensitive method for the quantitation of microgram quantities of protein utilizing the principle of protein-dye binding. *Anal Biochem* 1976; **72**: 248–254.

Supplementary Information accompanies this paper on Cell Death and Disease website (http://www.nature.com/cddis)